

# Description of Precipitation Retrieval Algorithm For ADEOS II AMSR

Guosheng Liu  
Florida State University

## 1. Basic Concepts of the Algorithm

This algorithm is based on Liu and Curry (1992, 1996), in which the rainfall rate is calculated from the combination of emission and scattering signatures. Beam-filling correction is embedded in the algorithm. Radiative transfer model tests show that it is not sensitive to the height of freezing level. This algorithm was tested in GPCP AIP-1, AIP-3, WetNet PIP-2 and PIP-3. The algorithm can retrieve rainfall over both ocean and land although slightly different formulations are used for the different surface types.

The AMSR algorithm is built on the SSM/I algorithm with conversions from AMSR brightness temperatures to SSM/I brightness temperatures.

*Ocean Algorithm:*

In this updated version, the combination function is defined by Liu et al. (1995) as following:

$$f = (1 - \frac{D}{D_0}) + 2(1 - \frac{PCT}{PCT_0}) \quad (1)$$

where  $D$  is the depolarization of 18.7 GHz and  $D_0$  is  $D$  at the threshold of rain onset;  $PCT$  is the polarization corrected brightness temperature defined by (Spencer et al., 1989):  $PCT = 1.818T_{B89V} - 0.818T_{B89H}$ , and  $PCT_0$  is  $PCT$  at the threshold of rain onset.  $PCT$  and  $D$  for AMSR channels are then converted to SSM/I  $PCT$  and  $D$  by the following equations:

$$\begin{aligned} PCT_{SSM/I} &= 2.2 + 0.996PCT_{AMSR} \\ D_{SSM/I} &= -0.14 + 0.903 * D_{AMSR} \end{aligned} \quad (2)$$

These equations are derived by radiative transfer simulations for various atmospheric and surface conditions. Then rainfall rate are calculated based on the equations originally derived from SSM/I channels.

$D_0$  and  $P_0$  are determined monthly for every  $3^\circ$  (latitude) x  $6^\circ$  (longitude) box based on 37 GHz depolarization and sea surface temperature, and are saved in a file as a look-up table. The relationship between  $f$  and rainfall rate is determined by radiative transfer calculation result with consideration of beam-filling effect, and can be expressed by

$$R = \alpha f^\beta \quad (3)$$

where  $\alpha$  and  $\beta$  are spatial scale-dependent coefficients. The dependence of  $\alpha$  and  $\beta$  on spatial scale is due to the spatial dependence of beam-filling effect. For SSM/I in which the spatial resolution of 19 GHz is  $\sim 50$  km,  $\alpha=10.6$  and  $\beta=1.621$ . For AMSR and TMI, the spatial resolution for 19 GHz is about half of that in SSM/I. The values for  $\alpha$  and  $\beta$  are determined by an empirical equation based on radiative transfer model simulation and TMI data:  $\alpha=8.25$ , and  $\beta=1.88$ . Test results show that these coefficients produce satisfactory rain rates from TMI data when compared to TRMM PR rain rates and GPCP climatology. Detailed discussion is given in section 2 on the scale-dependent parameters,  $\alpha$  and  $\beta$ .

*Land Algorithm:*

The land portion of our algorithm uses 18.7 and 89 GHz brightness temperatures. It is expressed by

$$R = a(DT_B - DT_{B0}) \quad (4)$$

where  $a=0.2$  is a coefficient derived from radiative transfer model simulations;  $DT_B=T_{B18.7}-T_{B89}$ . Again, we first convert  $DT_B$  for AMSR to  $DT_B$  for SSM/I by

$$DT_{BSSM/I} = -0.6 + 0.9558DT_{BAMSR} \quad (5)$$

Then the rainfall algorithm originally developed for SSM/I is used.

$DT_{B0}$  is  $DT_B$  at the threshold of rain onset that is determined monthly for every  $3^\circ$  (latitude) x  $6^\circ$  (longitude) box based on Liu and Curry (1992) and is saved in a file as a look-up table.

The algorithm is deterministic (non-iterative) and all threshold parameters ( $D_0$ ,  $PCT_0$ , and  $DT_{B0}$ ) are available as a look-up table. Therefore, the retrieval is extremely fast.

## 2. Determination of the Scale-Dependent Parameters

Results of earlier studies (e.g., Liu and Curry, 1992, Spencer et al., 1989) showed that the beam-filling effect tends to make the R- $T_B$  relation closer to “linear” than that indicated by radiative transfer models assuming a plane-parallel rain layer. Liu and Curry (1992) tried to explain this behavior of R- $T_B$  relation. The determination of  $\alpha$  and  $\beta$  in this algorithm is based on this consideration. First, we assume the parameter  $\beta$  in (3) varies with spatial scale,  $x$  (in km), as

$$\mathbf{b} = \mathbf{b}_\infty - A[1 - \exp(-Bx^\kappa)], \quad (6)$$

where  $\mathbf{b}_\infty=2.792$  is  $\beta$  for plain parallel rain layer determined by our radiative transfer simulations.  $\kappa$  is an adjustable parameter used to vary the strength of scale dependence. For now we use  $\kappa=0.7$  which seems to work well for our algorithm for TMI and SSM/I data.  $A$  and  $B$  are determined as following. First, when scale,  $x$ , becomes infinite large,  $\beta$  is 1, implying that for infinitely large spatial resolution the R- $T_B$  relation is linear (note the argument mentioned earlier). Then, it is determined that  $A = \mathbf{b}_\infty - 1$ . The constant  $B$  is then determined by applying (6) to our SSM/I algorithm used in Liu and Curry (1996), which gives  $\mathbf{b}_{SSM/I}=10.6$  for a scale of 50 km.

In the studies of Liu and Curry (1992), it is also found that when rainfall rate is as high as 50 mm/hr, the ratio between observed  $T_B$  and plane-parallel model generated  $T_B$  should be close to 1. Based on this argument, we determine  $\alpha$  by letting

$$\left( \frac{R_{50}}{\mathbf{a}_{AMSR}} \right)^{\frac{1}{\mathbf{b}_{AMSR}}} = \left( \frac{R_{50}}{\mathbf{a}_{SSM/I}} \right)^{\frac{1}{\mathbf{b}_{SSM/I}}} \quad (7)$$

where  $R_{50}=50$  mm/h.

It is noted that the development of the parameters of  $\alpha$  and  $\beta$  are based on the algorithm we developed for SSM/I. Figure 1 shows the f-R relations derived from the aforementioned approach for different spatial resolutions. For very high resolution, we may believe the rainfall within the FOV is homogenous. For very low resolution, the f-R relation is assumed to be linear. Actual satellite measurements (AMSR, TMI, SSM/I) will have an fR relation curve between the two extremes.

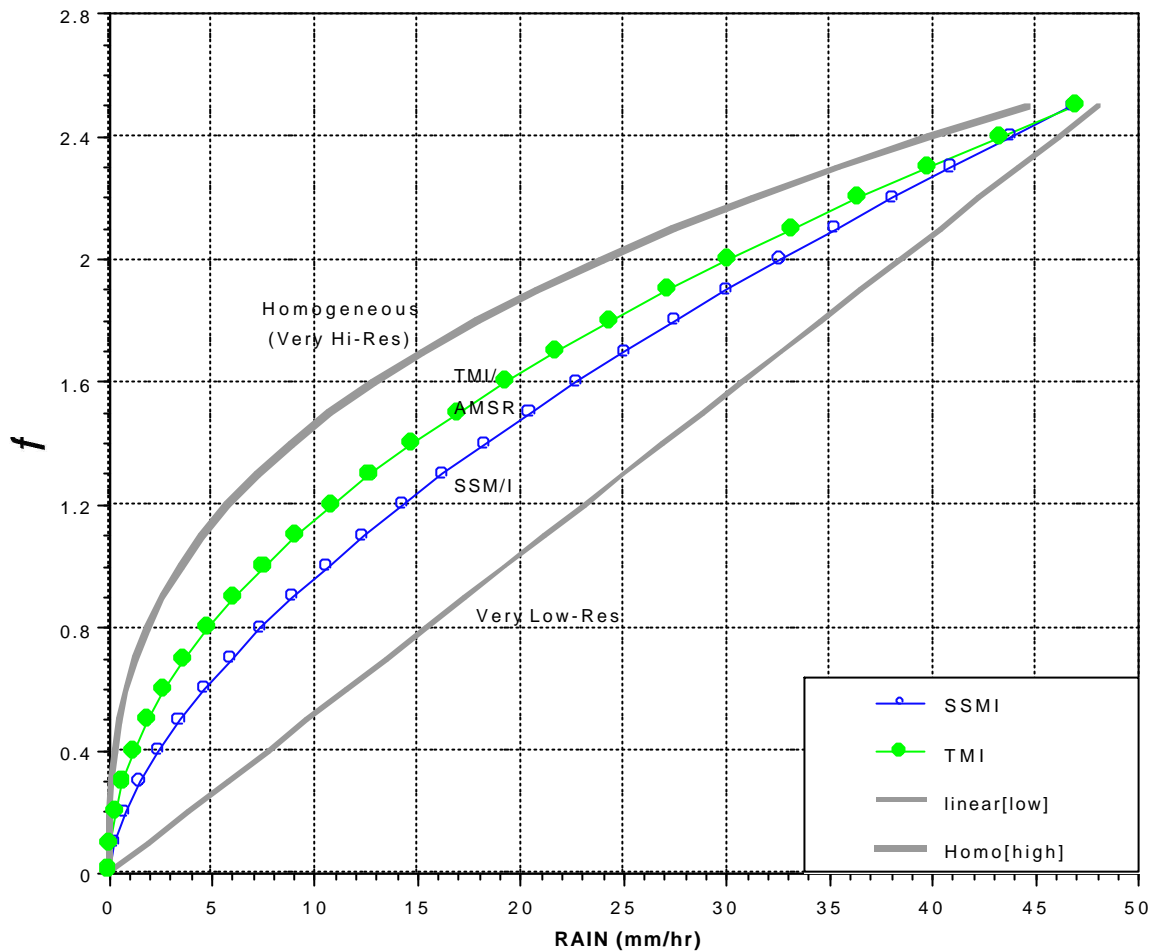


Fig. 1 Relations between  $f$  and rainfall rate for different spatial resolutions.

### 3. Validation -- Comparison with Other Datasets

Figure 2 shows the comparison of this algorithm using SSM/I data with GPCP satellite-raingauge combined monthly rainfall product (Huffman, et al., 1997) for the year of 1992. The two retrievals are generally agreed with each other although some discrepancies can also be found; such our retrievals are general lower, particularly for latitudes where precipitation peaks. This disagreement can partially be attributed to the low temporal coverage of SSM/I data.

Figure 3 shows the comparison with TRMM TMI-PR combined (3B31) product and GPCP satellite-raingauge combined product for 1998. Our retrievals seem to compare well with these products. We are still working on this comparison for other years to investigate whether there are discrepancies for those years. Further investigation may lead modification of the tuning parameter,  $\kappa$ , given in (6). Figure 4 shows the comparison with product derived from TRMM PR alone. The latitudinal variation of the two estimates agrees well although our estimates are slightly larger than the PR estimates. It is noted that PR estimates are also smaller than TRMM TMI and TRMM Combined products.

The following table lists the bias, correlation coefficient and rms difference when of our algorithm when compared to TRMM combined and GPCP products. The statistics are calculated using 1998 monthly  $5^\circ \times 5^\circ$  datasets.

Statistics When Compared to TRMM Combined and GPCP Data

	Bias in %	Correlation	rms Diff in %
GPCP	1%	0.78	69%
TRMM Combined	6%	0.82	61%

4. References

- Huffman, G. J., R. F. Adler, P.A. Arkin, A. Chang, R. Ferraro, A. Gruber, J. Janowiak, R.J. Joyce, A. McNab, B. Rudolf, U. Schneider, and P. Xie, 1997: The Global Precipitation Climatology Project (GPCP) Combined Precipitation Data Set. *Bull. Amer. Meteor. Soc.*, 78, 5-20.
- Liu, G., and J. A. Curry, 1992: Retrieval of precipitation from satellite microwave measurements using both emission and scattering. *J. Geophys. Res.*, **97**, 9959-9974.
- Liu, G., and J. A. Curry, 1996: Large-scale cloud features during January 1993 in the North Atlantic Ocean as determined from SSM/I and SSM/T-2 observations. *J. Geophys. Res.*, **101**,7019-7032.
- Liu, G., J. A. Curry and R. -S. Sheu, 1995: Classification of clouds over the western equatorial Pacific Ocean using combined infrared and microwave satellite data. *J. Geophys. Res.*, **100**, 13,811-13,826.
- Spencer, R. W., H M. Goodman, and R. E. Hood, 1989: Precipitation retrieval over land and ocean with SSM/I: Identification and characteristics of the scattering signal. *J. Atmos. Oceanic Technol.*, 6, 254-273

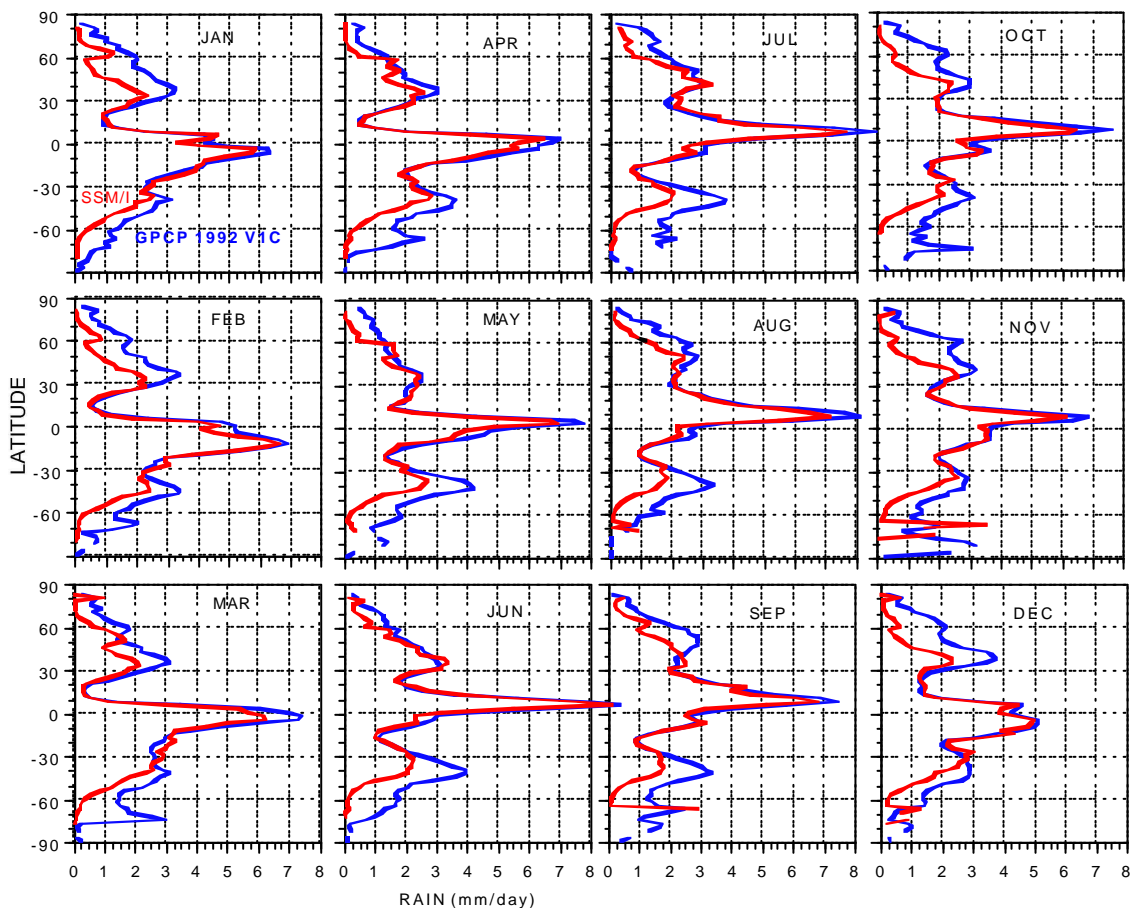


Fig. 2 Comparison with GPCP satellite-rain gauge combined rainfall(blue).

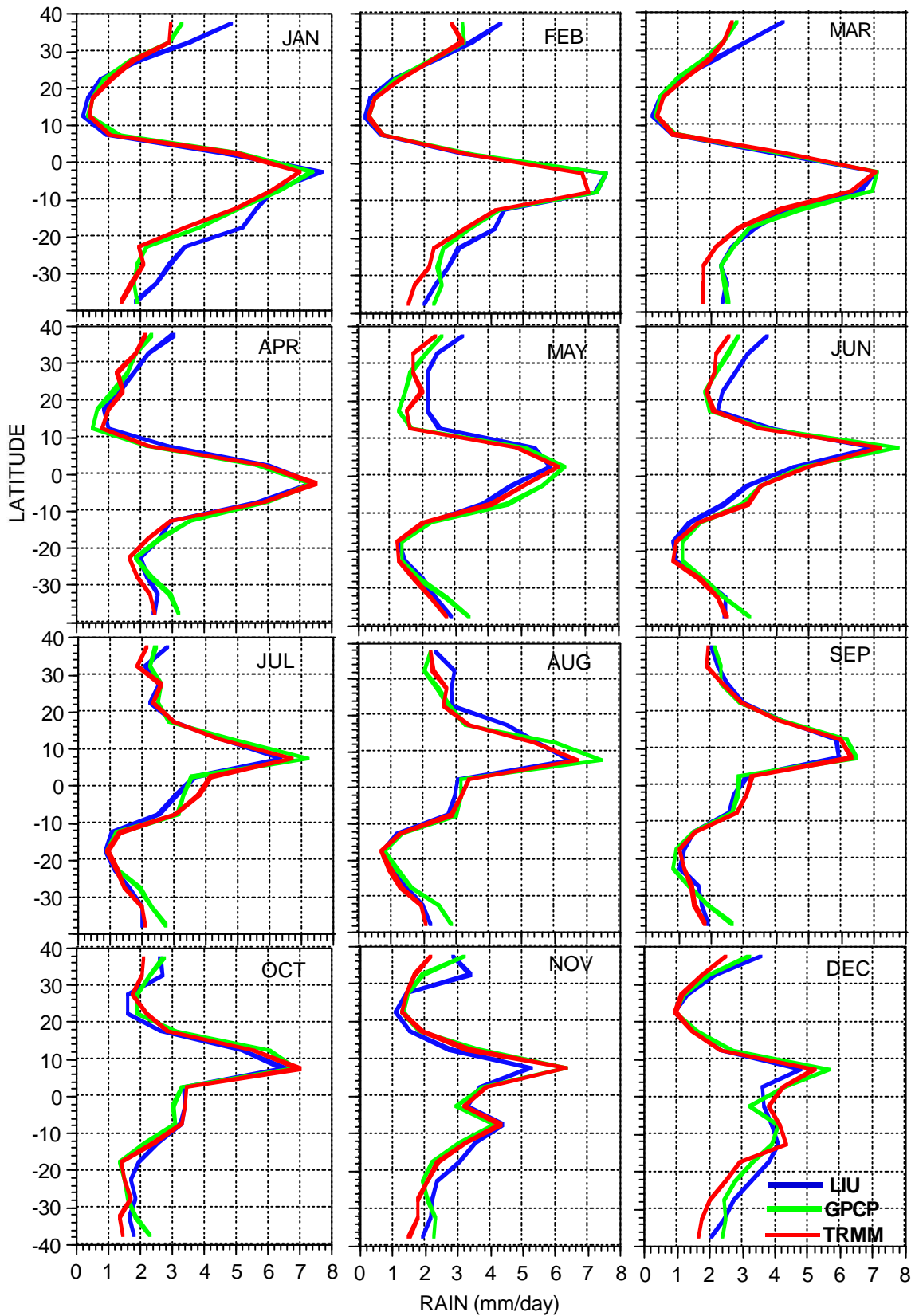


Fig.3 Comparison with TRMM combined (red) and GPCP (green) products for 1998.

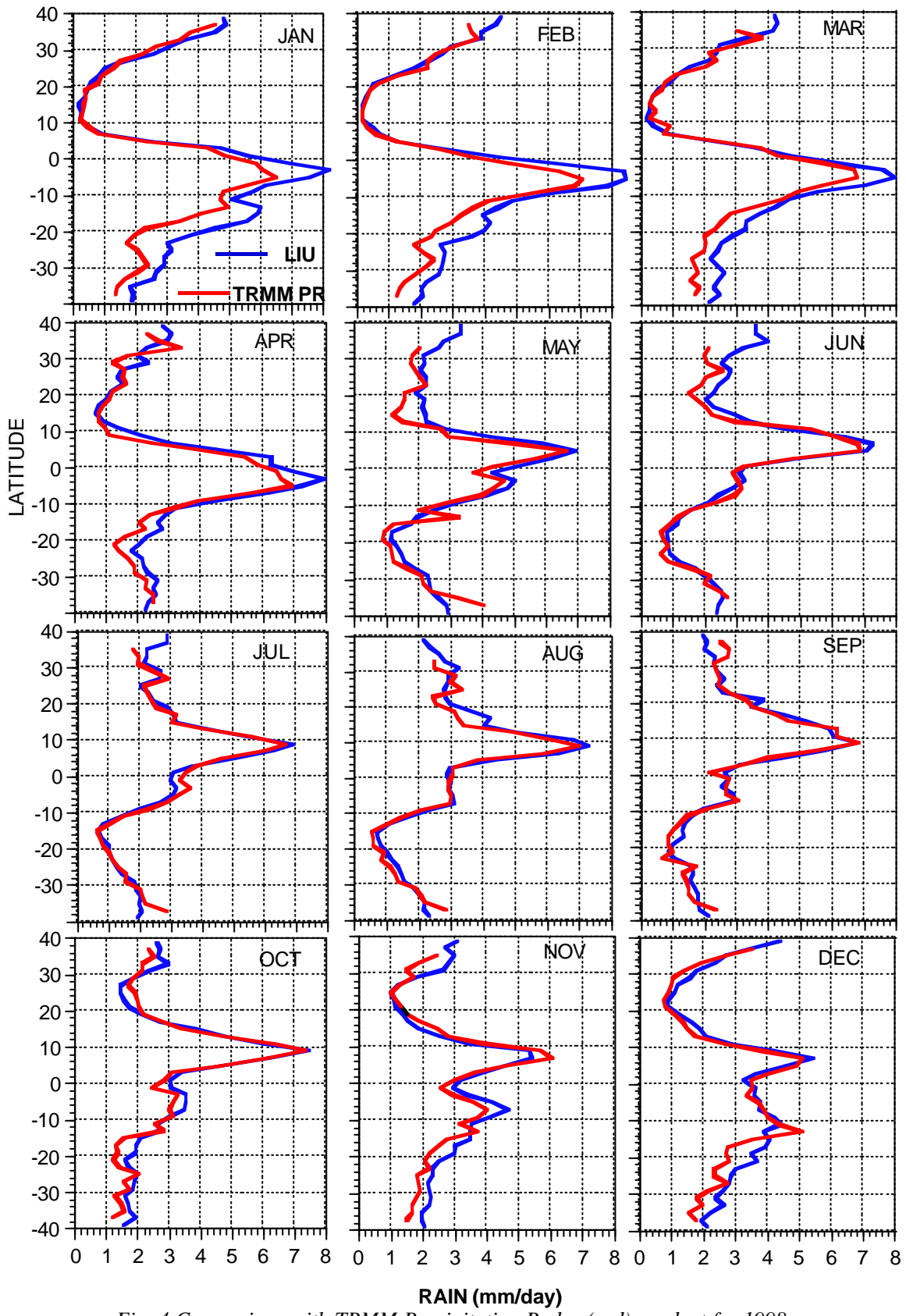


Fig. 4 Comparison with TRMM Precipitation Radar (red) product for 1998.